EFFECT OF CHARGE DIAMETER ON EXPLOSIVE PERFORMANCE

By Harry R. Nicholls and Wilbur I. Duvall

* * * * * * * * * * * * report of investigations 6806

UNITED STATES DEPARTMENT OF THE INTERIOR
Stewart L. Udall, Secretary

BUREAU OF MINES
Walter R. Hibbard, Jr., Director

This publication has been cataloged as follows:

Nicholls, Harry R

Effect of charge diameter on explosive performance, by Harry R. Nicholls and Wilbur I. Duvall. [Washington] U. S. Dept. of the Interior, Bureau of Mines [1966]

22 p. illus., tables. (U. S. Bureau of Mines. Report of investigations 6806)

Includes bibliography.

1. Explosives. I. Duvall, Wilbur Irving, 1915- , jt. auth. II. Title. (Series)

TN23.U7 no. 6806 622.06173

U. S. Dept. of the Int. Library

CONTENTS

ILLUSTRATIONS

TABLES

EFFECT OF CHARGE DIAMETER ON EXPLOSIVE PERFORMANCE

by

Harry R. Nicholls [1] and Wilbur I. Duvall [2]

ABSTRACT

The Bureau of Mines studied the effect of varying the diameter of explosive charges on the generation and propagation of strain waves. The parameters compared were strain amplitude, impulse, energy, and pulse shape. Three different explosives were detonated in three different charge diameters. Charges of cast 50/50 pentolite-detonated at the same velocity in 5-, 2.5-, and 1.5-inch diameters. Charges of ammonium nitrate-fuel oil prills and 45-percent semigelatin dynamite showed a strong detonation rate-diameter dependency. Detonation of these two explosives was considered nonideal. Differences in the diameter of the charge caused less difference in the strain-generating abilities of pentolite than in those of the other two explosives. This was also true for impulse and energy. Rise and fall times of the strain pulses for all three explosives were proportional to detonation time and cavity volume, respectively.

INTRODUCTION

The detonation rate of most commercial explosives varies with charge diameter. As charge diameter increases, detonation rate increases until some optimum detonation rate is reached. This optimum rate is generally known as the ideal detonation rate. The diameter at which ideal detonation occurs varies with explosive. For a 50/50 pentolite, with mass density of 1.62, ideal detonation occurs at a diameter of about 1 cm. For a 40 percent ammonia gelatin dynamite, the diameter is about 15 cm (2).[3]

[1]Former Bureau of Mines research geophysicist, Applied Physics Laboratory, College Park, Md.; now with Environmental Science Service Administration, Rockville, Md.

[2]Supervisory physicist, Denver Mining Research Center, Bureau of Mines, Denver, Colo.

[3]Underlined numbers in parentheses refer to items in the list of references at the end of this report.

Work on manuscript completed December 1965.

In both quarry and underground operations, shothole diameter can be increased or decreased. If the type of explosive is unchanged, an increase in diameter may effectively increase the strength of an explosive charge through an increase in detonation rate. Similarly, a decrease in diameter may result in a less powerful explosive because of a decrease in detonation rate. Such changes in explosive performance due to detonation rate--diameter dependency would differ from attendant changes due to a change in charge volume and charge geometry.

To study charge diameter effects, three different explosives were detonated in each of three different charge diameters. The explosives used were a cast 50/50 pentolite, a semigelatin dynamite (45-percent bulk strength), and a premixed ammonium nitrate-fuel oil (AN-FO) prill. These explosives were expected to have very slight, moderate, and strong detonation rate-diameter dependencies, respectively.

A total of 19 shots were detonated, 2 of each explosive in charge diameters of 1.5, 2.5, and 5 inches. One shot misfired, necessitating an additional test. Strain amplitude, impulse, energy, and pulse shape were studied for effects of charge diameter.

ACKNOWLEDGMENTS

The authors wish to express their appreciation to the Consolidated Quarries Division of the Georgia Marble Co., Lithonia, Ga., and in particular to Nelson Severinghaus, vice-president, and W. B. Hawkins, quarry superintendent, for providing the test site and assistance during the field portion of the program.

TEST SITE

The tests were conducted in a granite quarry near Lithonia, Ga. The quarry is within the Lithonia belt of granite-gneiss in the Piedmont Plateau of north-central Georgia. In hand samples, the rock appears to be a hard, firm, close-textured, fine-grained biotite granite-gneiss. The rock contains aplitic dikes and quartz and feldspar crystals up to 2 inches in diameter; it is relatively free of joints and fractures. In the absence of weathering, jointing, or fracturing, the rock is subjected to a horizontal static stress of 1,000 to 2,000 psi (4). Laboratory measurements indicate a high degree of anisotropy, but this is primarily between properties measured in a direction corresponding to an in situ vertical direction and any other orientation. Anisotropic effects are not generally evident in the type of field tests conducted in this investigation, nor are static stress conditions considered to be a contributing factor in the results obtained.

The weight density of the Lithonia granite-gneiss is 164 lb/ft^3. The longitudinal propagation velocity as determined in these tests is 18,500 ft/sec. The characteristic impedance (product of weight density and velocity) is 55 $lb/sec/in^3$.

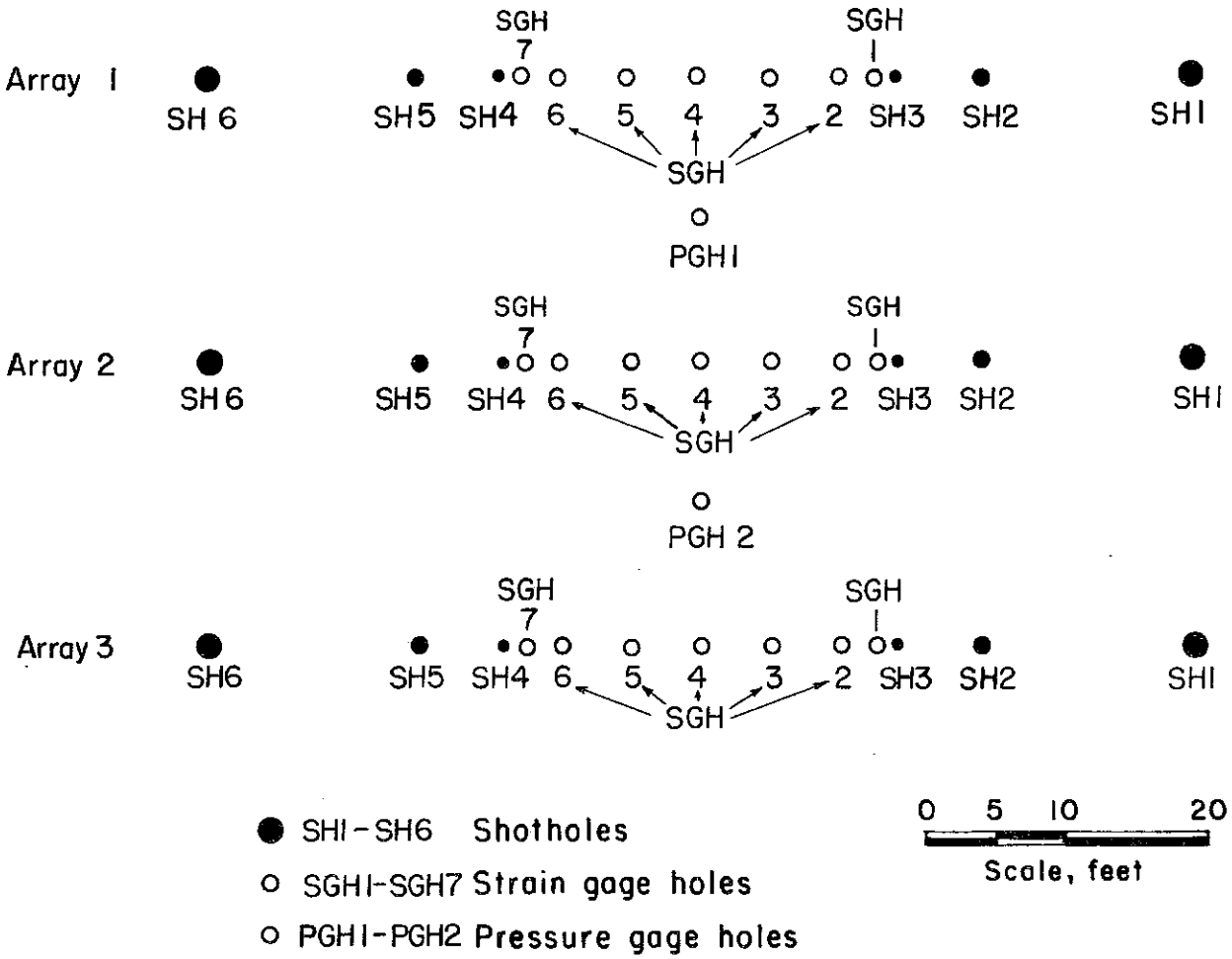

FIGURE 1. - Plan View of Test Arrays.

EXPERIMENTAL PROCEDURE

Three linear arrays of shotholes and gageholes were drilled as shown in the plan view of figure 1. The holes were drilled vertically to a depth such that the center of each gage and the center of gravity of each charge were on a horizontal datum plane about 29 feet below the surface. Holes SGH1 to SGH7 in each array and holes PGH1 and PGH2 between arrays were gageholes 3 inches in diameter. Holes SH1 to SH6 in each array were shotholes. In each array, SH1 and SH6 were 6 inches in diameter, SH2 and SH5 were 3 inches in diameter, and SH3 and SH4 were 1.9 inches in diameter.

Standard Bureau of Mines dynamic-type strain gages were installed in holes SGH1 to SGH7 in each array (6). These were oriented to respond to horizontal radial motion in their respective arrays and grouted in place with a Hydrocal[4] cement. Piezoelectric-type pressure gages were suspended in holes PGH1 and PGH2, which were water filled. The pressure gages were centered in the holes with mechanical spacing devices.

[4]Reference to specific brands is made for identification only and does not imply endorsement by the Bureau of Mines.

The output signals from all gages were carried by cable to a mobile laboratory which housed the recording equipment and accessory electronics. Gage output signals were amplified or attenuated as needed by a preamplifier system to deliver proper input voltages to a 14-channel FM magnetic tape recorder. The recordings were played back for analysis into a direct-writing oscillograph. The time scale of the final records for analysis was 625 μsec/in. The overall frequency response of the instrumentation system, including gages, was flat (± 12 percent) from 5 to 10,000 cps.

All explosive charges were 30 inches long. In each array there were two 1.5-inch-diameter, two 2.5-inch-diameter, and two 5-inch-diameter charges to be shot in 1.9-inch-, 3-inch-, and 6-inch-diameter holes, respectively, so that the coupling for all shots was nearly constant. Initiation for all shots was accomplished with an electric blasting cap and a 20-gram booster. Two shots of each diameter of each explosive were detonated for a total of 18 shots. The shots were randomized as much as possible to eliminate any systematic effects due to the rock or sequence of firing. The sequence of shooting in each array was from the outermost holes in towards the gageholes to preclude the propagation of energy through broken rock. After each shot, the resultant cavity was cleaned of crushed and broken material by directing a stream of compressed air of sufficient pressure and velocity to eject the crushed material from the drill hole. The cavity was then measured by adding known increments of sand and measuring the buildup in the hole.

The pentolite and semigelatin dynamite charges were encased in cardboard wrappers during their manufacture. To insure similarity in shooting conditions and to maintain constant coupling (80 to 83 percent), the AN-FO prills were packaged in similar cardboard containers at the site. This is not the condition under which prills are normally shot because confinement is usually complete. However, prills were chosen for use simply as an explosive which had a strong diameter effect, and the results should not be considered as an evaluation of the explosives themselves.

The detonation rate of each charge was measured. Two chronograph contactors were inserted in each charge, one 6 inches above the point of the detonation and the second 1.5 feet from the first. Contactors are simple make circuits with which appropriate electronic circuitry is used to operate the start-stop sections of a microsecond timer. The quotient of the distance interval divided by the time interval is the detonation rate. In addition, detonation rates were measured continuously. The continuous probe consists of 2-foot-long threaded nylon rod, wrapped with Nichrome resistance wire. The wire-wrapped nylon rod is encased in a thin-wall aluminum shell and inserted in the charge. The probe is powered by a constant current source. As detonation proceeds, the aluminum shell collapses and continuously shorts out the threaded wire. The resultant varying resistance causes a voltage drop across the gage. This voltage change is displayed versus time on an oscilloscope and photographed. The slope of the photographed trace is proportional to the detonation rate.

Zero times for shot-to-gage arrival time measurements were established by placing a chronograph contactor at the point of initiation in each charge.

The voltage output from the contactor make circuit was recorded on one of the FM tape channels.

A great deal of extraneous electrical noise was evident on the strain data from the first three shots in the test series. Such noise is often referred to as firing hash or shot noise because it originates at the instant of charge detonation. Many things were tried before each of the first three shots in an attempt to eliminate the electrical pickup, including additional grounding and isolation of signal and fire line cables. Prior to the fourth shot, the sand stemming and sides of the shothole were moistened with water. This completely eliminated the electrical noise problem and became standard procedure for the balance of the tests. However, data from shot S1 were completely unusable because of the noise. Only two data points from shot S3 were usable. All data from shot S2 were poor but usable. Gage SG3 in array 3 did not function properly for any shot in the array, and no data were obtained from that gage.

DATA AND ANALYSIS

Explosive Properties

Table 1 gives the explosive properties. The weight and detonation rates of each charge were measured in the field. Data from the two charges of each diameter were averaged. Detonation pressures were calculated using Brown's approximate formula (1):

$$P = 2.16 \times 10^{-4}\ \rho g\ D^2\ [0.45/(1 + 0.0128\ \rho g)],$$

where P = detonation pressure, psi,

ρg = weight density, lb/ft^3,

and D = detonation velocity, ft/sec.

The decrease in weight density with decrease in charge diameter reflects the increase in relative percentage of weight that the wrapper represents for smaller diameter charges. The relative increase in percentage of voids in the pentolite charges to receive probes and contactors is also reflected by a decrease in weight density with decreased charge diameter.

TABLE 1. - Explosive properties

Explosive	Symbol	Charge diam, inches	Charge volume, ft^3	Weight, pounds	Weight density, lb/ft^3	Detonation rate, ft/sec	Detonation pressure, psi x 10^6
Cast 50/50 pentolite.	Pent	5	0.340	34.8	102	24,600	2.60
		2.5	.0852	8.1	95.1	24,700	2.54
		1.5	.0307	2.8	91.3	24,500	2.46
Semigelatin dynamite, 45-percent bulk strength.	SG45	5	.340	27.3	80.3	18,100	1.26
		2.5	.0852	6.6	77.5	16,200	.991
		1.5	.0307	2.3	75.0	15,600	.903
Premixed AN-FO prill.	AN-FO	5	.340	19.3	56.7	9,900	.313
		2.5	.0852	4.6	54.0	8,100	.204
		1.5	.0307	1.6	52.2	7,400	.167

Shooting Sequence

Table 2 gives the shooting sequence employed. The number preceding the explosive represents the order of the shot in the overall sequence. The coding for shot numbers in this report is, first, number of shot in sequence; second, array number; third, shothole number. Thus, the ninth shot in the test series was AN-FO prills in array 1 shothole SH3 and would be referred to as shot S9-A1-SH3.

TABLE 2. - Order of shooting

Hole	Diameter, inches	Array 1		Array 2		Array 3	
		Shot	Explosive	Shot	Explosive	Shot	Explosive
SH1.....	5	S7	SG45	S14	AN-FO	S1	Pent
SH2.....	2.5	S8	Pent	S15	SG45	S3	AN-FO
SH3.....	1.5	S9	AN-FO	S19	Pent	S6	SG45
SH4.....	1.5	S12	Pent	S18	SG45	S5	AN-FO
SH5.....	2.5	S11	SG45	S17	AN-FO	S4	Pent
SH6.....	5	S10	AN-FO	S16	Pent	S2	SG45

Pressure Data

The pressure gages in holes PGH1 and PGH2 were used throughout the tests beginning with shot S4-A3-SH5. In a previous test series (5), large differences existed in strain amplitudes among arrays independent of distance or explosive-type considerations. The pressure gages used in these tests were nearly omnidirectional; therefore, they were expected to give similar amplitudes for identical charges from two shots of the same explosive for identical travel distances providing no real array effect existed. Table 3 shows all the pressure gage data. Of the direct comparisons available, only those from shots S5-A3-SH4 and S9-A1-SH3 show any significant difference (1.79 psi versus 0.98 psi and 5.86 psi versus 2.55 psi). This is presumably because of the generally poor quality of the data from these two shots. On the basis of these comparisons, no array effect was detected. None was evident in the strain data.

Strain Data

The tracings of strain pulses shown in figure 2 illustrate the measurements made on the strain pulses. The initial portion of the trace prior to the arrival of the pulse is the zero base line. Deflection above the baseline is compressive strain, deflection below is tensile strain, and time increases from left to right. Type a strain pulse was obtained most often in the test series. Type b typifies the strain pulse obtained at shot-to-gage distances of 15 feet or less where the rock experiences permanent compressive deformation. Type c illustrates the strain pulses obtained from the 2.5- and 1.5-inch-diameter AN-FO charges. The contribution due to the booster was an appreciable portion of the total strain pulses. To facilitate analysis, a smooth curve, shown as a dashed line, was drawn through type c pulses. The hatched portion, E, was assumed to be a strain pulse produced by the booster and excluded from all calculations and analysis.

TABLE 3. - Pressure amplitudes, psi[1]

	Gage PG1	Gage PG2
Shots with Pent:		
S16-A2-SH6	-	71.4
S4-A3-SH5	30.1A	-
S8-A1-SH2	74.7	33.1A
S12-A1-SH4	70.1B	20.1
S19-A2-SH3	62.1B	59.8B
Shots with SG45:		
S7-A1-SH1	39.5	25.9
S15-A2-SH2	25.0C	23.1C
S11-A1-SH5	33.7C	16.4
S6-A3-SH3	7.25	17.1D
S18-A2-SH4	17.2D	17.1D
Shots with AN-FO:		
S10-A1-SH6	19.0E	13.6
S14-A2-SH1	13.8E	13.1E
S17-A2-SH5	4.48F	4.42F
S5-A3-SH4	1.79G	5.86H
S9-A1-SH3	2.55H	.98G

[1]A through H following numbers indicate that data are directly comparable. For example the 30.1 psi registered by shot S4-A3-SH5 at gage PG1 and the 33.1 psi registered by shot S8-A1-SH2 at gage PG2 both are followed by the letter A, indicating that travel distance, charge type, and geometry were the same. Gages PG1 and PG2 were equidistant from all array 2 shotholes; thus, array 2 data for each shot are comparable.

In addition to direct measurement of the quantities shown in figure 2, all strain data were processed on a semiautomatic digitizing system for computer calculation of impulse and energy. Impulse is proportional to the integral of the strain pulse with respect to time and was handled in two parts: compressive impulse, impulse of the compressive portion or first half cycle; and total impulse, impulse of the first cycle. Energy is proportional to the integral of strain squared as a function of time and was also treated in two parts: compressive and total energy. Tensile strain was determined only as a step in determining fall strain (sum of compressive and tensile strain). The importance of fall strain in rock breakage was pointed out in a previous report (3).

Tables 4, 5, and 6 give arrival times and times associated with various parts of the pulse as illustrated in figure 2. Tables 7, 8, and 9 give amplitude, impulse, and energy data from all the shots.

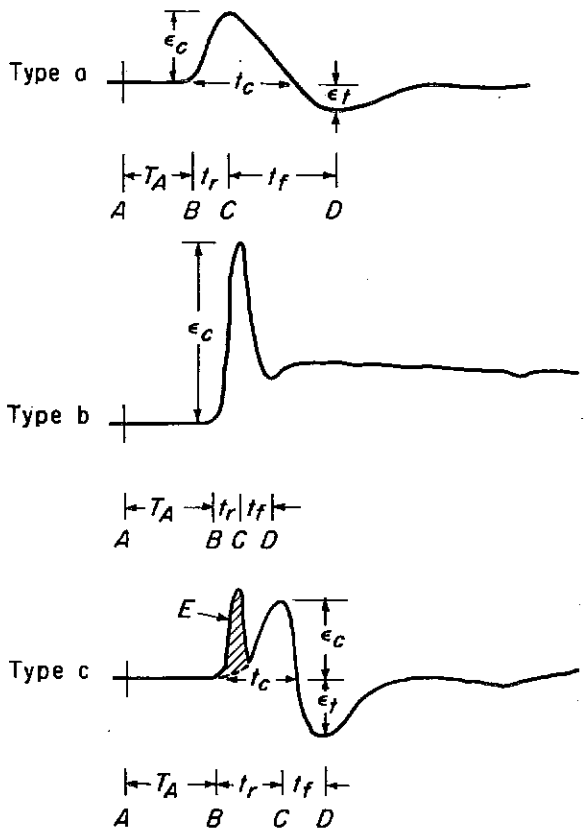

A	Detonation of charge	t_r	Rise time
B	Start of strain pulse	t_c	Compression time
C	Peak compressive strain	t_f	Fall time
D	End of fall strain	ϵ_c	Peak compressive strain
E	Portion due to booster	ϵ_t	Tensile strain
T_A	Arrival time of pulse		

FIGURE 2. - Typical Strain Pulses.

The horizontal longitudinal propagation velocity determined statistically from arrival time-distance data was 18,500 ±350 ft/sec. This was the common slope for all shots.

Figures 3 and 4 are plots of rise and fall time versus distance (R) respectively. The appropriate times are shown individually for each explosive. No statistical analysis has been made of these data. Figure 3 clearly indicates the dependency of rise time on the detonation rate or detonation time. For pentolite, which has a constant detonation rate within experimental error, a smooth curve could be drawn through the data. There is a slight increase in rise time with increased distance, which may indicate absorption. For semigelatin dynamite, more scatter is apparent. However, it is generally true that the rise time at any given distance is shorter from a large diameter shot, indicating the rise time-detonation rate dependency. This effect is most pronounced for the AN-FO prills which have the slowest detonation rate and the greatest detonation rate-diameter effect.

Plots of fall time versus distance for each explosive are shown in figure 4. These plots exhibit a different phenomenon. Fall time has been associated with the size of cavity created by the detonation of the charge (7).

TABLE 4. - Arrival time and pulse shape data, pentolite

Gage	Shot-to-gage distance, R, feet	Arrival time, T_A, msec	Rise time, t_r, msec	Compression time, t_c, msec	Fall time, t_f, msec
Shot S16-A2-SH6, 5-Inch Diameter					
SG1.....	95	5.181	0.151	0.445	0.529
SG2.....	90	4.907	.134	.462	.521
SG3.....	80	4.349	.151	.474	.576
SG4.....	70	3.795	.139	.434	.578
SG5.....	60	3.257	.126	.441	.584
SG6.....	50	2.693	.117	.450	.517
SG7.....	45	2.404	.113	.411	.525
Shot S4-A3-SH5, 2.5-Inch Diameter					
SG1.....	65	3.500	0.129	0.306	0.335
SG2.....	60	3.216	.121	.322	.335
SG4.....	40	2.135	.125	.305	.293
SG5.....	30	1.606	.101	.281	.285
SG6.....	20	1.044	.101	.302	.256
SG7.....	15	.805	.096	.297	.287
Shot S8-A1-SH2, 2.5-Inch Diameter					
SG1.....	15	0.810	0.084	0.304	0.261
SG2.....	20	1.096	.093	.257	.299
SG3.....	30	1.615	.114	.278	.291
SG4.....	40	2.166	.118	.281	.294
SG5.....	50	2.699	.139	.298	.428
SG6.....	60	3.232	.126	.319	.416
Shot S12-A1-SH4, 1.5-Inch Diameter					
SG1.....	53	2.870	0.121	0.234	0.293
SG2.....	48	2.594	.113	.234	.221
SG3.....	38	2.068	.104	.230	.200
SG4.....	28	1.527	.092	.204	.192
SG5.....	18	.996	.092	.229	.200
SG6.....	8	.446	.079	.354	-
SG7.....	3	.183	-	-	-
Shot S19-A2-SH3, 1.5-Inch Diameter					
SG1.....	3	0.210	0.071	-	-
SG2.....	8	.461	.084	-	-
SG3.....	18	1.014	.096	0.222	0.272
SG4.....	28	1.532	.108	.212	.221
SG5.....	38	2.088	.096	.222	.260
SG6.....	48	2.612	.122	.256	.235
SG7.....	53	2.909	.113	.252	.231

TABLE 5. - Arrival time and pulse shape data, semigelatin dynamite

Gage	Shot-to-gage distance, R, feet	Arrival time, T_A, msec	Rise time, t_r, msec	Compression time, t_c, msec	Fall time, t_f, msec
Shot S2-A3-SH6, 5-Inch Diameter					
SG1.....	95	5.206	0.171	0.338	0.488
SG2.....	90	4.935	.138	.372	.522
SG4.....	70	3.808	.163	.405	.367
SG5.....	60	3.297	.180	.380	.347
SG6.....	50	2.729	.138	.380	.380
SG7.....	45	2.487	.121	.380	.414
Shot S7-A1-SH1, 5-Inch Diameter					
SG1.....	45	2.489	0.122	0.375	0.624
SG2.....	50	2.755	.131	.397	.557
SG3.....	60	3.287	.156	.413	.603
SG4.....	70	3.830	.143	.400	.619
SG5.....	80	4.360	.144	.422	.608
SG6.....	90	4.888	.160	.447	.570
Shot S11-A1-SH5, 2.5-Inch Diameter					
SG1.....	65	3.498	0.185	0.295	0.227
SG2.....	60	3.237	.152	.257	.227
SG3.....	50	2.697	.152	.274	.227
SG4.....	40	2.177	.118	.249	.232
SG5.....	30	1.637	.100	.263	.259
Shot S15-A2-SH2, 2.5-Inch Diameter					
SG1.....	15	0.821	0.092	0.281	0.281
SG2.....	20	1.076	.096	.289	.264
SG3.....	30	1.633	.142	.297	.251
SG4.....	40	2.165	.130	.290	.218
SG5.....	50	2.711	.147	.290	.269
SG6.....	60	3.249	.160	.299	.307
SG7.....	65	3.544	.164	.303	.295
Shot S6-A3-SH3, 1.5-Inch Diameter					
SG1.....	3	0.186	0.080	-	-
SG2.....	8	.440	.085	0.309	-
SG4.....	28	1.481	.114	.275	0.216
SG5.....	38	2.052	.117	.269	.214
SG6.....	48	2.623	.113	.259	.234
SG7.....	53	2.865	.159	.267	.171
Shot S18-A2-SH4, 1.5-Inch Diameter					
SG1.....	53	2.855	0.210	0.310	0.188
SG2.....	48	2.595	.189	.281	.180
SG3.....	38	2.071	.176	.272	.189
SG4.....	28	1.518	.105	.272	.235
SG5.....	18	.951	.109	.278	.278
SG6.....	8	.391	.097	-	-
SG7.....	3	.114	.101	-	-

TABLE 6. - Arrival time and pulse shape data, AN-FO prills

Gage	Shot-to-gage distance, R, feet	Arrival time, T_A, msec	Rise time, t_r, msec	Compression time, t_c, msec	Fall time, t_f, msec
	Shot S10-A1-SH6, 5-Inch Diameter				
SG1.....	95	5.166	0.211	0.389	0.253
SG2.....	90	4.828	.291	.465	-
SG3.....	80	4.414	.173	.334	-
SG4.....	70	3.797	.182	.397	.325
SG5.....	60	3.259	.223	.408	.337
SG6.....	50	2.711	.211	.413	.446
	Shot S14-A2-SH1, 5-Inch Diameter				
SG1.....	45	2.479	0.262	0.385	0.254
SG2.....	50	2.716	.296	.419	.263
SG3.....	60	3.291	.254	.402	.292
SG4.....	70	3.782	.238	.379	.297
SG5.....	80	4.315	.284	.436	.283
SG6.....	90	4.848	.275	.448	.326
SG7.....	96	5.148	.271	.440	-
	Shot S3-A3-SH2, 2.5-Inch Diameter				
SG1.....	15	0.837	0.322	0.368	-
SG2.....	20	1.117	.289	.314	-
	Shot S17-A2-SH5, 2.5-Inch Diameter				
SG1.....	65	3.515	0.360	0.498	-
SG2.....	60	3.268	.372	.485	0.197
SG3.....	50	2.729	.318	.460	.264
SG4.....	40	2.189	.301	.447	.255
SG5.....	30	1.638	.333	.458	.229
SG6.....	20	1.079	.308	.500	.325
SG7.....	15	.792	.317	.513	.329
	Shot S5-A3-SH4, 1.5-Inch Diameter				
SG1.....	53	2.857	0.601	0.832	0.634
SG2.....	48	2.574	.672	1.059	.596
SG4.....	28	1.489	.634	.947	.559
SG5.....	18	.956	.647	-	-
	Shot S9-A1-SH3, 1.5-inch Diameter				
SG1.....	3	0.202	-	-	-
SG2.....	8	.459	-	-	-
SG3.....	18	1.019	-	-	-
SG4.....	28	1.544	0.372	1.280	-
SG5.....	38	2.094	.358	.822	0.838
SG6.....	48	2.604	.367	.792	.754
SG7.....	53	2.911	-	-	-

TABLE 7. - Strain amplitude, impulse, and energy data, pentolite

Gage	Shot-to-gage distance, R, feet	Compressive strain, ϵ_c, μin/in	Fall strain, ϵ_f, μin/in	Compressive impulse, I_c, μin sec/in x 10^4	Total impulse, I_t, μin sec/in x 10^4	Compressive energy, E_c, $(\mu in/in)^2$ sec x 10^6	Total energy, E_t, $(\mu in/in)^2$ sec x 10^6
Shot S16-A2-S6, 5-Inch Diameter							
SG1	95	51.4	68.0	1.19	0.470	0.442	0.525
SG2	90	62.5	82.4	1.32	.444	.580	.692
SG3	80	60.4	76.6	1.31	.542	.544	.629
SG4	70	68.2	84.4	1.32	.395	.598	.708
SG5	60	107	130	2.12	1.00	1.62	1.78
SG6	50	135	160	2.66	2.03	2.46	2.54
SG7	45	150	183	2.65	-	2.73	3.04
Shot S4-A3-SH5, 2.5-Inch Diameter							
SG1	65	47.4	62.4	0.726	0.195	0.253	0.695
SG2	60	58.9	75.4	.853	.233	.345	.961
SG4	40	99.0	126	1.59	.875	1.21	3.06
SG5	30	166	192	2.11	1.39	2.51	6.00
SG6	20	276	296	3.65	3.27	7.00	16.0
SG7	15	439	-	-	-	-	-
Shot S8-A1-SH2, 2.5-Inch Diameter							
SG1	15	414	451	6.05	5.89	17.6	17.7
SG2	20	235	257	3.03	2.57	5.49	5.57
SG3	30	162	191	2.28	1.46	2.74	2.87
SG4	40	97.1	110	1.40	.999	1.02	1.05
SG5	50	78.4	97.5	1.09	.436	.651	.733
SG6	60	48.8	60.8	.723	.260	.261	.295
Shot S12-A1-SH4, 1.5-Inch Diameter							
SG1	53	32.5	47.0	0.404	0.154	0.0955	0.123
SG2	48	44.3	58.3	.476	.217	.145	.171
SG3	38	49.5	64.7	.566	.210	.206	.248
SG4	28	64.2	87.5	.714	.218	.339	.413
SG5	18	133	155	1.49	.827	1.41	1.52
SG6	8	270	-	4.12	-	7.90	-
Shot S19-A2-SH3, 1.5-Inch Diameter							
SG1	3	1,180	-	13.8	-	126	-
SG2	8	384	-	5.0	-	12.5	-
SG3	18	121	136	1.33	0.928	1.18	3.93
SG4	28	51.4	69.5	.579	-	.224	-
SG5	38	45.0	56.9	.515	.215	.171	.626
SG6	48	25.4	34.3	.313	.0890	.0589	.232
SG7	53	22.6	30.8	.289	.104	.0489	.188

TABLE 8. - Strain amplitude, impulse, and energy data, semigelatin dynamite

Gage	Shot-to-gage distance, R, feet	Compressive strain, ϵ_c, μin/in	Fall strain, ϵ_f, μin/in	Compressive impulse, I_c, μin sec/in x 10^4	Total impulse, I_t, μin sec/in x 10^4	Compressive energy, E_c, $(\mu in/in)^2$ sec x 10^6	Total energy, E_t, $(\mu in/in)^2$ sec x 10^6
Shot S2-A3-SH6, 5-Inch Diameter							
SG1	95	34.0	44.8	0.730	0.166	0.185	0.231
SG2	90	38.1	50.9	.825	.200	.239	.297
SG4	70	57.6	73.1	1.23	.413	.540	.633
SG5	60	66.8	84.1	1.34	.271	.663	.801
SG6	50	88.5	110	1.77	.637	1.14	1.31
SG7	45	85.2	109	1.75	.584	1.14	1.32
Shot S7-A1-SH1, 5-Inch Diameter							
SG1	45	114	137	2.15	0.783	1.78	2.02
SG2	50	88.3	113	1.71	.645	1.08	1.25
SG3	60	74.9	96.9	1.64	.580	.935	1.08
SG4	70	58.4	72.2	1.20	.430	.512	.596
SG5	80	51.5	64.9	1.13	.305	.438	.521
SG6	90	34.8	45.0	.810	.187	.204	.252
Shot S11-A1-SH5, 2.5-Inch Diameter							
SG1	65	23.0	35.9	0.384	0.128	0.0698	0.0921
SG2	60	32.4	47.7	.364	.0456	.0686	.0939
SG3	50	34.5	49.1	.527	.153	.143	.179
SG4	40	41.1	55.5	.604	.200	.196	.243
SG5	30	63.4	88.7	1.01	.374	.520	.625
Shot S15-A2-SH2, 2.5-Inch Diameter							
SG1	15	139	163	2.20	1.79	2.32	2.38
SG2	20	89.1	106	1.41	.977	.923	.978
SG3	30	43.5	53.7	.764	.589	.269	.280
SG4	40	27.7	36.2	.464	.246	.0994	.113
SG5	50	25.1	34.9	.431	.0650	.0869	.112
SG6	60	18.0	26.1	.314	.0389	.0440	.0606
SG7	65	14.6	21.3	.237	-	.0261	.0374
Shot S6-A3-SH3, 1.5-Inch Diameter							
SG1	3	592	-	-	-	-	-
SG2	8	146	-	3.01	-	3.65	-
SG4	28	27.8	45.1	.463	0.227	.105	0.135
SG5	38	17.5	27.7	.305	.127	.0449	.0575
SG6	48	12.0	19.9	.204	.0482	.0210	.0292
SG7	53	10.4	17.1	.167	.0620	.0141	.0196
Shots S18-A2-SH4, 1.5-Inch Diameter							
SG1	53	10.2	16.5	0.180	-	0.0144	0.0234
SG2	48	10.9	19.0	.190	-	.0164	.0268
SG3	38	12.2	19.7	.221	-	.0220	.0332
SG4	28	19.4	33.1	.357	-	.0573	.0890
SG5	18	38.5	56.0	.700	-	.228	.275
SG6	8	141	-	-	-	-	-
SG7	3	523	-	-	-	-	-

TABLE 9. - Strain amplitude, impulse, and energy data, AN-FO prills

Gage	Shot-to-gage distance, R, feet	Compressive strain, ϵ_c, μin/in	Fall strain, ϵ_f, μin/in	Compressive impulse, I_c, μin sec/in x 10^4	Total impulse, I_t, μin sec/in x 10^4	Compressive energy, E_c, $(\mu in/in)^2$ sec x 10^6	Total energy, E_t, $(\mu in/in)^2$ sec x 10^6
Shot S10-A1-SH6, 5-Inch Diameter							
SG1	95	14.9	21.5	0.354	0.0793	0.0413	0.0527
SG2	90	16.5	23.6	.397	.0748	.0480	.0642
SG3	80	17.7	31.6	.373	--	.0489	.128
SG4	70	25.2	34.1	.581	.141	.110	.138
SG5	60	31.6	42.7	.751	.192	.181	.225
SG6	50	31.4	40.8	.813	.311	.201	.237
Shot S14-A2-SHL, 5-Inch Diameter							
SG1	45	40.5	55.5	0.938	0.193	0.287	0.352
SG2	50	34.0	46.9	.793	.183	.205	.256
SG3	60	22.9	32.3	.521	-	.0896	.122
SG4	70	17.9	26.1	.398	-	.0529	.0736
SG5	80	17.2	23.9	.411	.0981	.0934	.0680
SG6	90	13.7	19.4	.346	.104	.0364	.0461
SG7	95	13.7	19.8	.348	.0481	.0364	.0501
Shot S3-A3-SH2, 2.5-Inch Diameter							
SG1	15	38.4	-	0.529	-	0.132	-
SG2	20	19.6	-	.297	-	.0430	-
Shot S17-A2-SH5, 2.5-Inch Diameter							
SG1	65	3.86	7.00	0.104	0.0268	0.00288	0.00471
SG2	60	4.09	7.07	.110	.0374	.00325	.00482
SG3	50	4.28	7.40	.100	-	.00312	.00508
SG4	40	5.67	10.2	.113	-	.00475	.00888
SG5	30	11.5	17.1	.243	.138	.0204	.0248
SG6	20	19.2	24.6	.412	.330	.0565	.0595
SG7	15	30.6	40.8	.650	.493	.137	.147
Shot S5-A3-SH4, 1.5-Inch Diameter							
SG1	53	0.833	1.89	0.0261	-	0.000130	0.000443
SG2	48	1.09	1.60	.0610	0.0410	.000546	.000658
SG4	28	2.89	4.33	.121	.0696	.00231	.00282
SG5	18	7.02	-	-	-	-	-
Shot S9-A1-SH3, 1.5-Inch Diameter							
SG4	28	3.89	2.91	0.197	0.0501	0.00505	0.00505
SG5	38	2.38	2.60	.0856	.0101	.00137	.00153
SG6	48	1.81	-	.0591	-	.000630	.000847

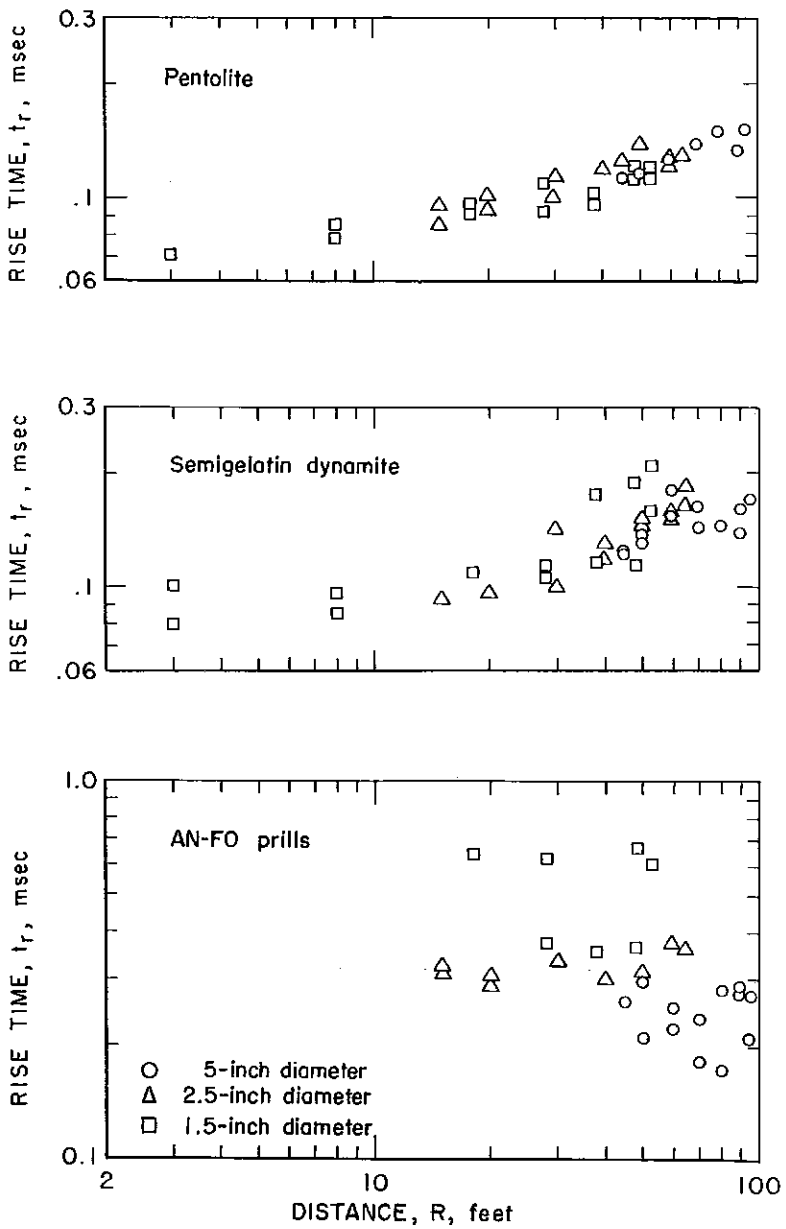

FIGURE 3. - Rise Time Versus Distance.

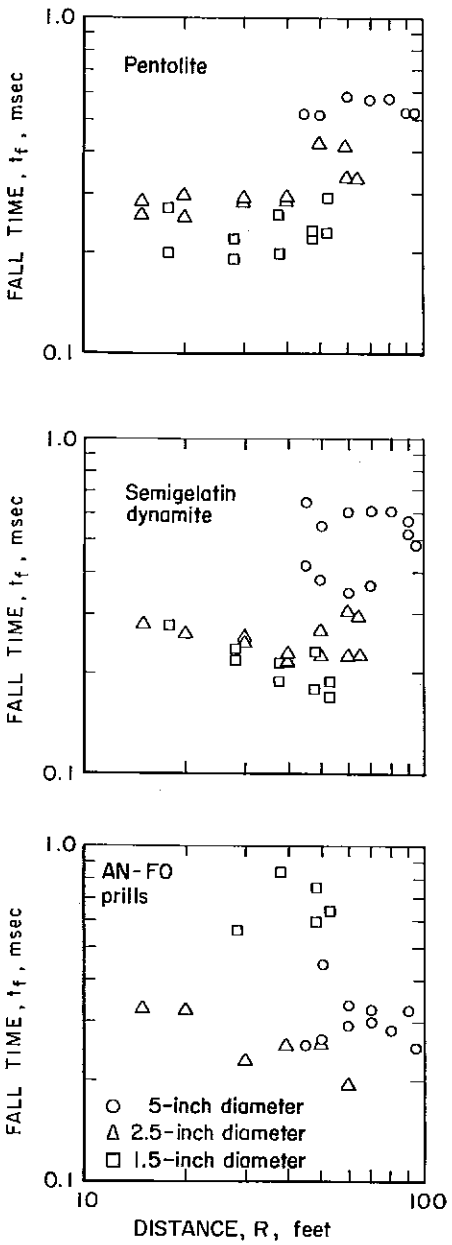

FIGURE 4. - Fall Time Versus Distance.

Average Cavity Size

Table 10 gives the average cavity size (volume of rock broken) from each explosive in each diameter. Comparing cavity size from the table with relative fall times indicates that for a given explosive, longer fall times correlate with larger cavities. It is also true among explosives that larger cavity sizes may be correlated with longer fall times. The only exception is from the 1.5-inch-diameter charges of AN-FO prills which are probably subjected to the most error due to reflected wave arrivals.

TABLE 10. - Average cavity size, ft^3

Explosive charge diameter, inches	Pentolite	Semigelatin dynamite	AN-FO prills
5.....	2.75	1.84	1.01
2.5.....	.53	.60	.27
1.5.....	.17	.11	.04

Data Analysis

All strain amplitude, impulse, and energy data were treated statistically to determine common slopes and individual intercepts for each parameter. Straight lines were fitted to the data by using an equation of the form

$$Y = KR^{-n}$$

where K = intercept at $R = 1$,

n = decay exponent or slope of regression curve,

and R = distance.

Y represents the parameter under study. Thus Y is one of the following: peak compressive strain (ε_c), fall strain (ε_f), compressive impulse (I_c), total impulse (I_t), compressive energy (E_c), and total energy (E_t).

Figures 5 through 10 are plots of the data for each parameter versus distance. The data from each explosive type has been shown separately in each figure. Table 11 is a summary of intercept and slopes of the data shown in the previous figures. The missing values include data from shot 1 omitted because of noise. In other sets only two reliable data points existed for a

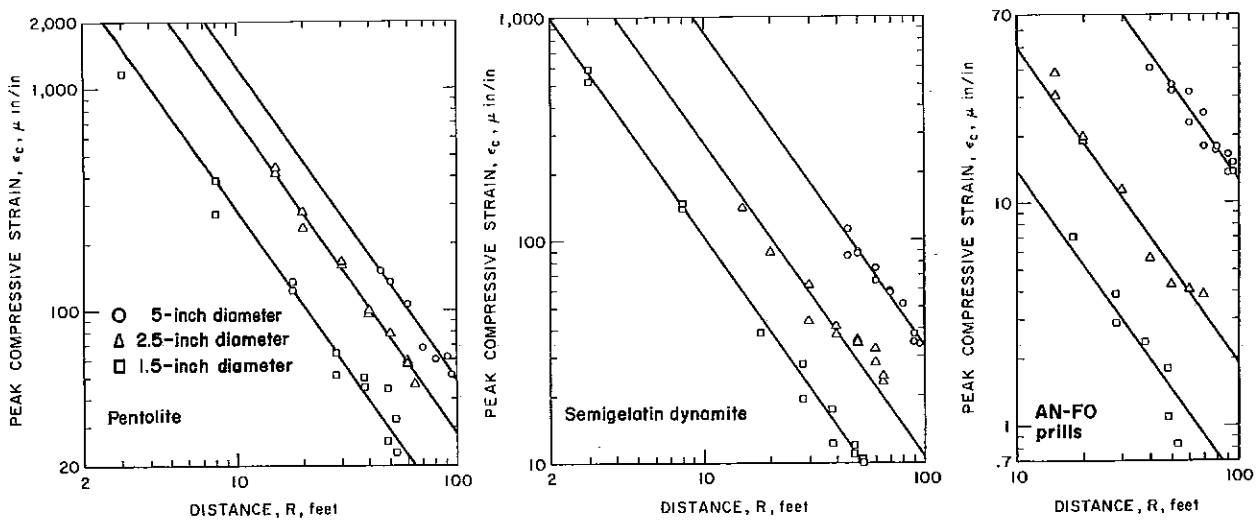

FIGURE 5. - Peak Compressive Strain Versus Distance.

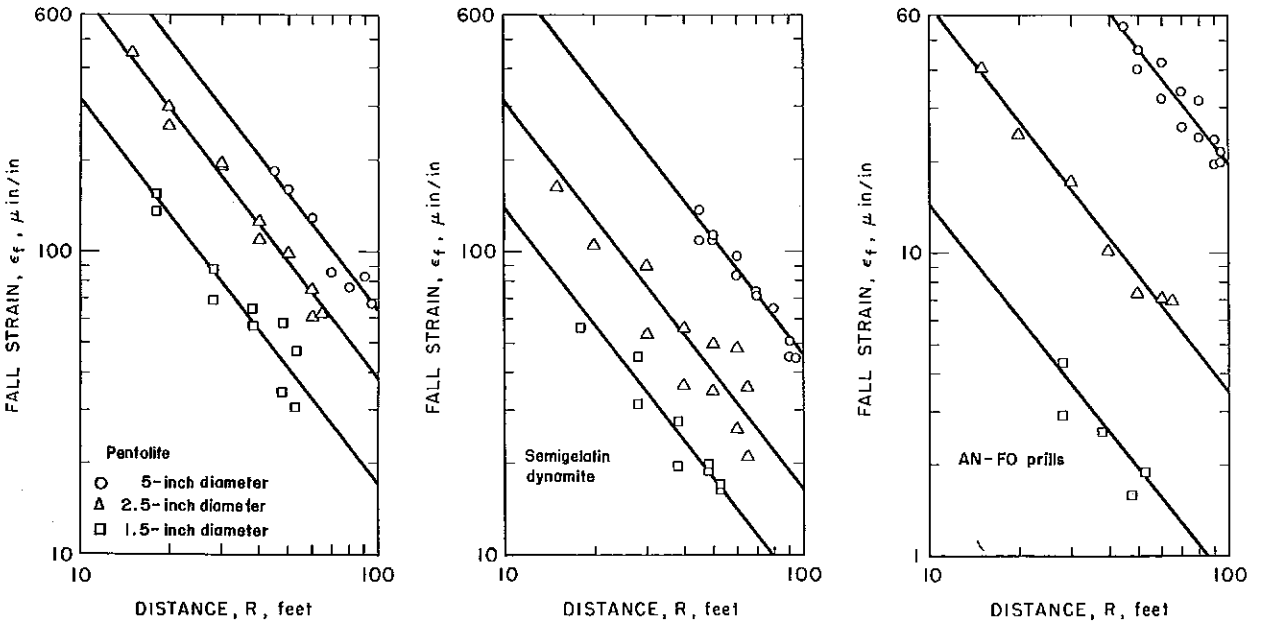

FIGURE 6. - Fall Strain Versus Distance.

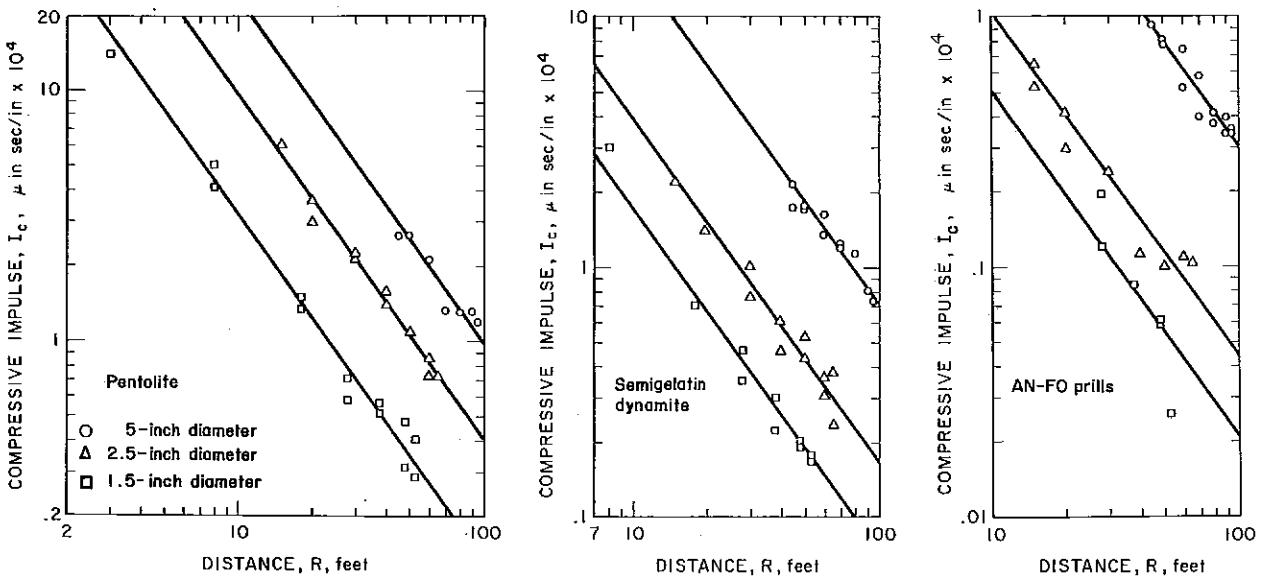

FIGURE 7. - Compressive Impulse Versus Distance.

parameter for a given shot; the data points are shown in the figures but not included in the table because two data points cannot be treated statistically.

TABLE 11. - Summary of intercepts and slopes

Charge diameter, inches	K x 10^4 μin/in		K x 10^6 μin sec/in		K x 10^8 (μin/in)^2 sec	
	Peak 13 strain, n = -1.40 ±0.02	Fall strain, n = -1.27 ±0.09	Compressive impulse, n = -1.37 ±0.03	Total impulse, n = -2.11 ±0.09	Compressive energy, n = -2.74 ±0.06	Total energy, n = -0.55 ±0.06
Pentolite						
5.....	-	-	-	-	-	-
5.....	3.12	2.24	5.49	6.42	1,010	522
Average.	3.12	2.24	5.49	6.42	1,010	522
2.5.....	1.85	1.37	2.29	1.65	262	335
2.5.....	1.75	1.29	2.20	1.75	249	139
Average.	1.80	1.33	2.25	1.70	256	237
1.5.....	.764	.684	8.14	.458	38.4	26.6
1.5.....	.631	.513	6.81	.402	27.6	53.7
Average.	.698	.599	.748	.430	33.0	40.2
Semigelatin Dynamite						
5.....	2.07	1.55	3.76	2.29	494	270
5.....	2.24	1.64	4.11	2.85	581	310
Average.	2.16	1.60	3.94	2.57	538	290
2.5.....	.831	.720	.936	.513	52.3	32.1
2.5.....	.559	.460	.905	.442	31.0	18.9
Average.	.695	.590	.921	.478	41.7	25.5
1.5.....	.284	.287	.443	.237	8.99	5.73
1.5.....	.237	.235	.366	-	5.91	4.56
Average.	.260	.260	.405	.237	7.45	5.15
AN-FO Prills						
5.....	0.895	0.730	1.83	1.12	105	67.4
5.....	.787	.635	1.60	.842	80.7	47.9
Average.	.841	.683	1.72	.981	92.9	57.7
2.5.....	-	-	-	-	-	-
2.5.....	.125	.122	.251	.180	1.94	1.38
Average.	.125	.122	.251	.180	1.94	1.38
1.5.....	.0290	.0271	.096	-	.144	.124
1.5.....	.0412	-	.142	-	.255	.185
Average.	.0351	.0271	.119	-	.250	.155

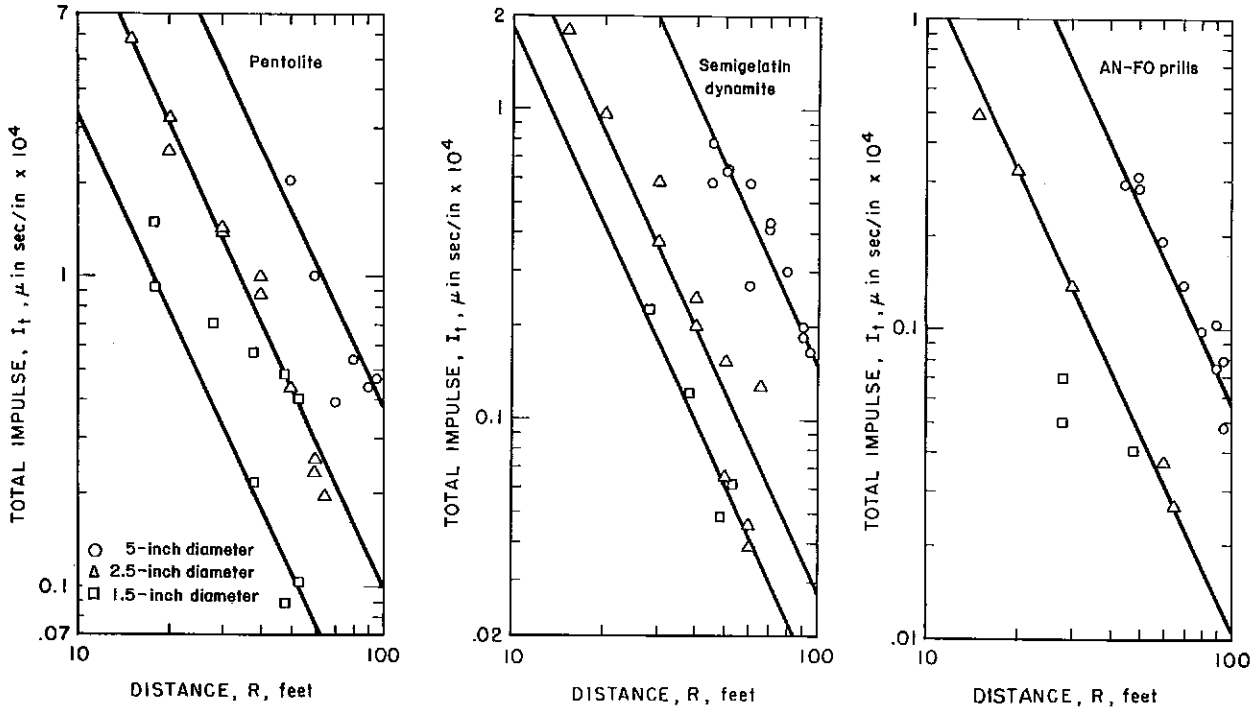

FIGURE 8. - Total Impulse Versus Distance.

Examination of table 11 indicates that an effect considerably greater than that expected from detonation rate-diameter dependency is present. First, consider peak strain within and between explosives. Peak compressive strain is less by a factor of 4 from 1.5-inch-diameter shots than from 5-inch-diameter shots of pentolite. The detonation rate and pressure are virtually the same. Included, then, in the fourfold reduction are effects due to charge size and geometry. No scaling was applied to the data. Under similar conditions, reductions by factors of about 8 and 24 are evident in data from semigelatin dynamite and AN-FO prills, respectively, when charge diameter is reduced from 5 to 1.5 inches. The excess above the fourfold reduction observed in pentolite data indicates a significant decrease in strain-generating ability for small-diameter nonideal explosive charges. Also it should be noted that 5-inch-diameter charges of all these explosives show only a fourfold change in peak strain intercept for large changes in detonation rate and pressure. The lesser change in rate and pressure for the different diameter charges of semigelatin dynamite and AN-FO prills produce much larger changes in peak strain intercept. Similar comparisons are apparent in the various other parameters.

CONCLUSIONS

Small-diameter explosive charges which detonate under nonideal conditions are much less effective than larger diameter charges of the same explosive in producing strain waves in rock than would be predicted solely from the decreased detonation rate and pressure. The loss in efficiency is greater than effects due to charge size and geometry.

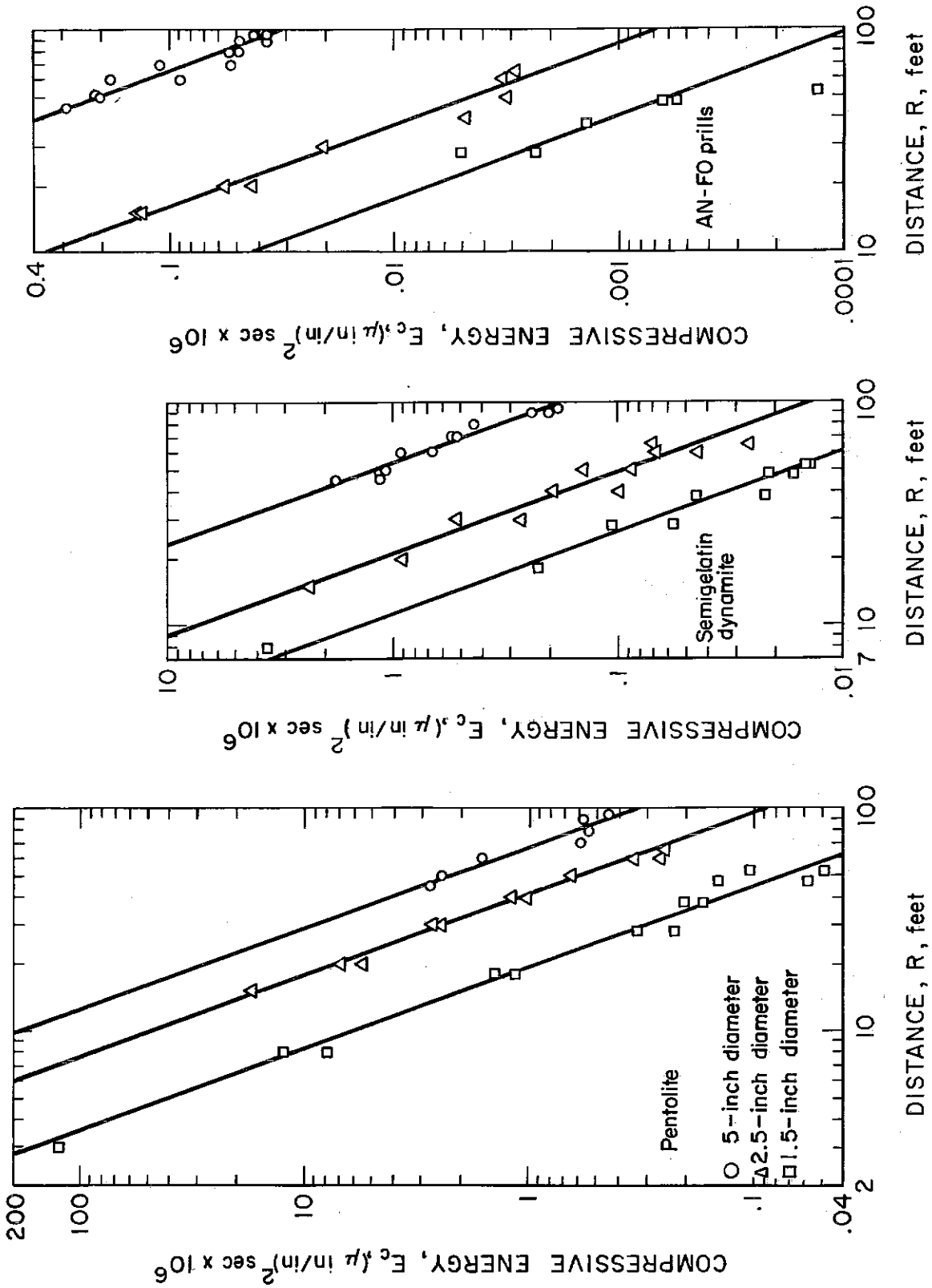

FIGURE 9. - Compressive Energy Versus Distance.

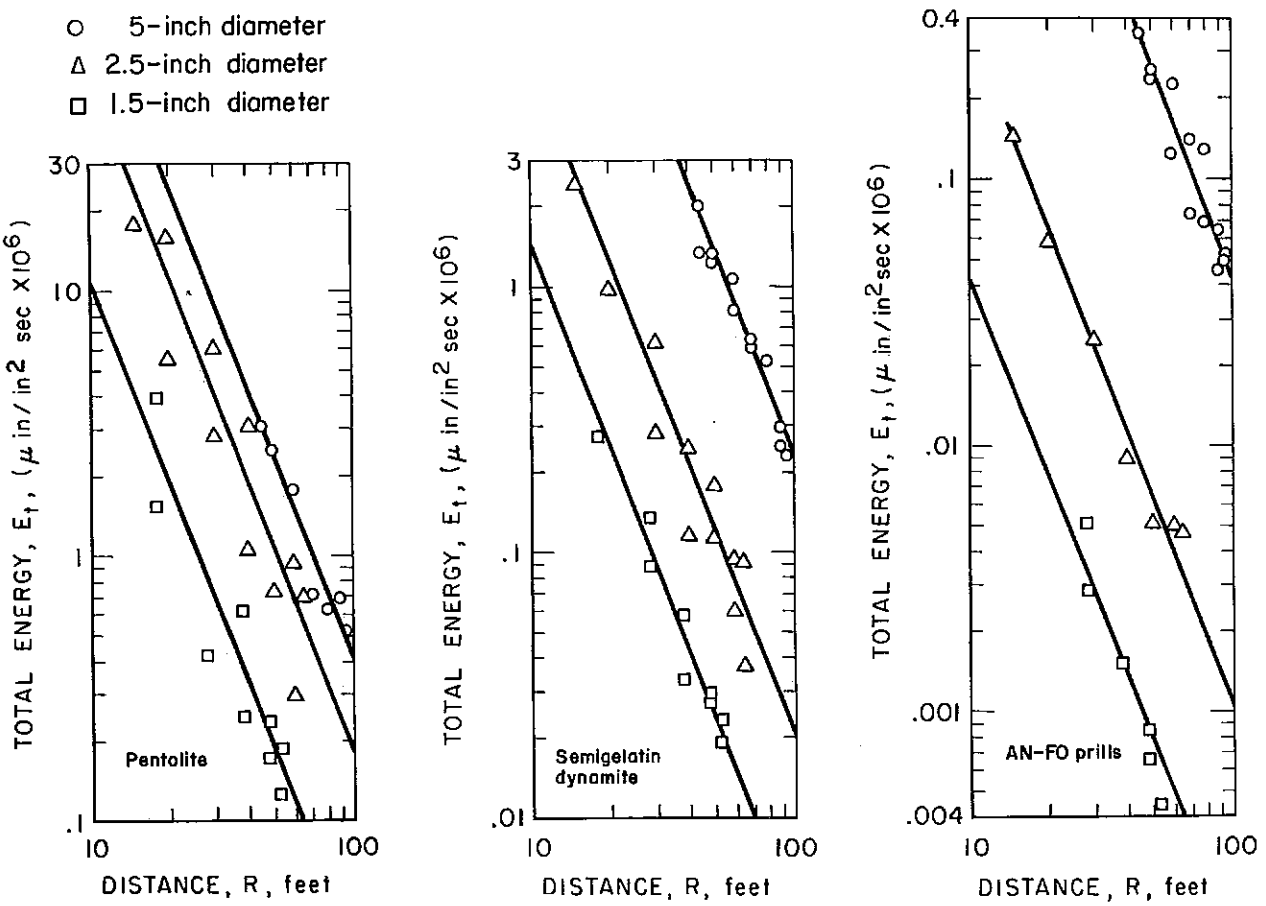

FIGURE 10. - Total Energy Versus Distance.

On the basis of the test results, changes in charge diameter under practical mining or quarrying conditions should receive the utmost consideration. Increases in charge diameter while maintaining constant explosive type and spacing may increase efficiency but could also result in overshooting and overbreak. Decreases in charge diameter with the same explosive and spacing appear to produce losses in efficiency greater than changes in charge size, geometry, and detonation rate-pressure would produce if nonideal detonation occurs.

REFERENCES

1. Brown, R. F. Determination of Basic Performance Properties of Blasting Explosives. Ch. in First Symposium on Rock Mechanics. Colorado Sch. Mines Quart., v. 51, No. 3, July 1956, pp. 171-188.

2. Cook, Melvin A. The Science of High Explosives. Reinhold Publishing Corp., New York, 1958, pp. 44-59.

3. Duvall, Wilbur I., and Thomas C. Atchison. Rock Breakage By Explosives. BuMines Rept. of Inv. 5356, 1957, 52 pp.

4. Hooker, Verne E., Harry R. Nicholls and Wilbur I. Duvall. In Situ Stress Determinations in a Lithonia Gneiss Outcrop. Earthquake Notes, v. 35, Nos. 3-4, September-December 1964, p. 46.

5. Nicholls, Harry R., Lyle W. Colburn, Thomas R. Bur, and Thomas E. Slykhouse. Comparison of Two Methods for Studying Relative Performance of Explosives in Rock. BuMines Rept. of Inv. 6888 (in Press).

6. Obert, Leonard, and Wilbur I. Duvall. A Gage and Recording Equipment for Measuring Dynamic Strain in Rock. BuMines Rept. of Inv. 4581, 1949, 11 pp.

7. Sharpe, J. A. The Production of Elastic Waves by Explosion Pressure, Part I. Theory and Empirical Field Observations. Geophysics, v. 7, No. 2, 1942, pp. 144-154.

INT.-BU.OF MINES,PGH.,PA. 9815